Bulletin of the Seismological Society of America, 90, 2, pp. 275–285, April 2000

Interpretation of Seismic Vertical Amplification Observed at an Array Site

by Jun Yang and Tadanobu Sato

Abstract Strong ground motions were recorded at Port Island, Kobe, by a borehole array during the 1995 Hyogo-ken Nanbu (Kobe) earthquake. These records indicate that, while the horizontal peak accelerations were reduced as seismic waves traveling from the bottom to the surface, motions in the vertical direction were significantly amplified at the surface, with peak value of 1.5 to 2 times larger than the horizontal components. Some studies have discussed local site effects on the horizontal motions, whereas the available study on the vertical amplification is limited. In this article, we present a possible mechanism to explain the observed vertical amplification in detail. We consider that the observed large vertical amplification is mainly associated with incomplete saturation of near-surface soils, which causes substantial amplification of *P* waves but does not affect the propagation of *S* waves. Based on the concept of homogeneous pore fluid and Biot's theory of two-phase media, we discuss the characteristics of *P*-wave velocity, Poisson's ratio and degree of saturation in shallow soil layers, and show evidence of incomplete saturation of near-surface soils at the array site. We analyze a simple model to theoretically investigate the effects of saturation on vertical-motion amplification. The results show that the degree of saturation may produce substantial influence on the amplification, both amplitude and frequency content. Using a solid-fluid coupled finite element procedure, we perform a simulation of the observed vertical motions at the array site by including the effects of saturation. The results demonstrate the mechanism of large amplification caused by incomplete saturation of near-surface layers. The present study indicates that vertical-component motions may significantly be affected by pore-water saturation of soils, suggesting that we may need to carefully examine the condition of saturation in the study of vertical site amplification.

Introduction

During the 1995 Hyogo-ken Nanbu (Kobe) earthquake ($M_w = 6.9$), strong ground motions were recorded at Port Island, Kobe, by a borehole array which consisted of four triaxial accelerometers located at the surface and three different depths. Figure 1 shows the three-component accelerograms at the surface and the depth of 83 m (the location of the deepest accelerometer). The distribution of peak accelerations with depth in three components is given in Figure 2. These records indicate that, while the peak amplitudes in both horizontal-component motions (E-W and N-S, respectively) were reduced as seismic waves traveled from the bottom to the surface, the vertical motions were greatly amplified at the surface, with peak value of 556 cm/s^2, which was about 1.5 to 2.0 times larger than the horizontal components. So far some studies have discussed the characteristics of horizontal motions and concluded that the reduction of peak accelerations in horizontal components was associated with soil nonlinearity and liquefaction in surface reclaimed layers (e.g., Sato *et al.*, 1996; Aguirre and Irikura, 1997; Kokusho and Matsumoto, 1999; Yang *et al.*, 2000). In particular, Yang *et al.* (2000) addressed the correlation of the characteristics of horizontal motions with the stress-strain histories and the build-ups of excess pore-water pressure in subsurface soils, which were simulated using an effective-stress-based nonlinear finite element procedure. On the other hand, the array records indicate that the effects of soil nonlinearity on vertical-component motions seem to be small, as supported by some inversion analyses (e.g., Sato *et al.*, 1996). Probably because the compression modulus is larger than the corresponding shear modulus and because of the vertical confinement, nonlinear soil behavior is expected to occur for larger excitations in the vertical than the horizontal component, as suggested by Trifunac and Todorovska (1996) for interpreting the vertical peak accelerations recorded during the 1994 Northridge earthquake.

As mentioned before, one particular feature of the array records is that a large amplification of vertical motion was observed at the surface. Although considerable interest has been given to the nonlinear effects on horizontal motions, the available study on the mechanism of the large vertical amplification is limited. To address this issue would be of interest not only from the viewpoint of explanation of this site-specific phenomenon, but also in potential applications in site evaluation using a technique known as H/V, which involves the analysis of spectral ratios for horizontal and vertical components and assumes that vertical components do not change with site response (Nakamura, 1989; Lermo and Chavez-Garcia, 1993; Theodulidis and Bard, 1995).

Taking into account the general understanding that peak accelerations in seismograms are probably carried by body waves while long-period arrivals are surface waves (Boore and Smith, 1999), one may expect that the observed substantial vertical amplification is probably related to the characteristic of low *P*-wave velocity in near-surface layers of the site. In order to find the major contribution to the vertical-motion amplification, we calculate the spectral ratios of the recorded vertical accelerations at the surface and at a depth of 83 m, which may well represent the transfer function for the site considered. As shown in Figure 3, significant amplification took place at frequencies around of 4.5 to 5.5 Hz. It could be impossible to generate surface waves with such high frequencies due to the effects of basin edge. Both two- and three-dimensional simulations of ground motions by including local topography (Kawase, 1996; Kawase and Hayashi, 1996; Pitarka *et al.*, 1998) suggested that large amplification caused by the basin-edge effects took place at periods greater than 1 sec and in a narrow zone offset less than 1 km from the basin edge (obviously Port Island is located outside of this zone). In addition, due to soil liquefaction and associated substantial nonlinearity in shallow layers at the site, shear waves, especially high-frequency contents, were strongly attenuated as they traveling through

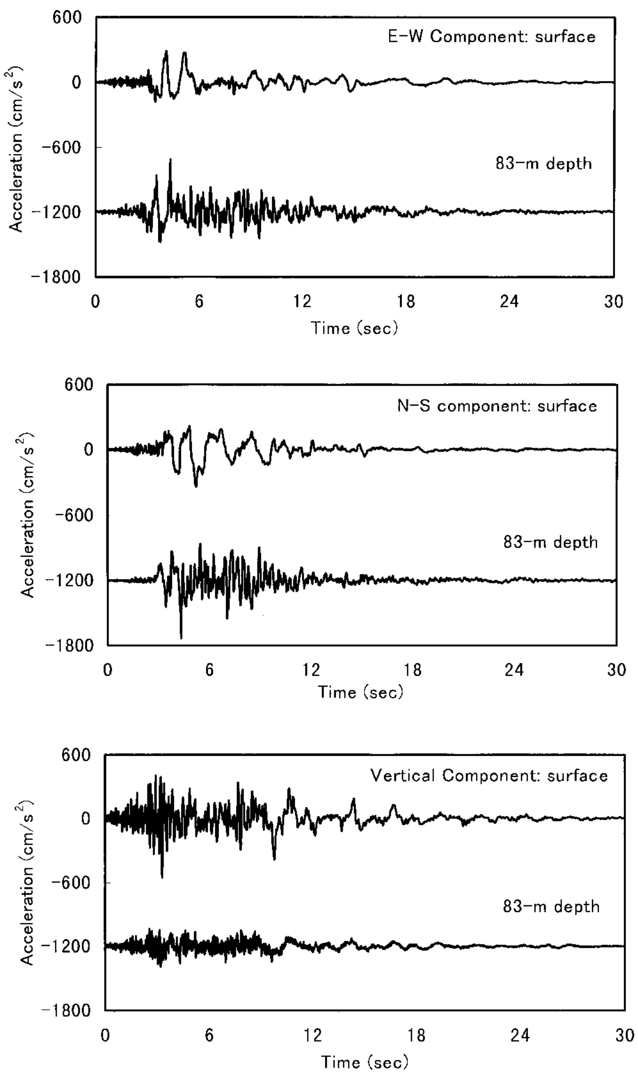

Figure 1. Three-component accelerograms at the surface and 83-m depth.

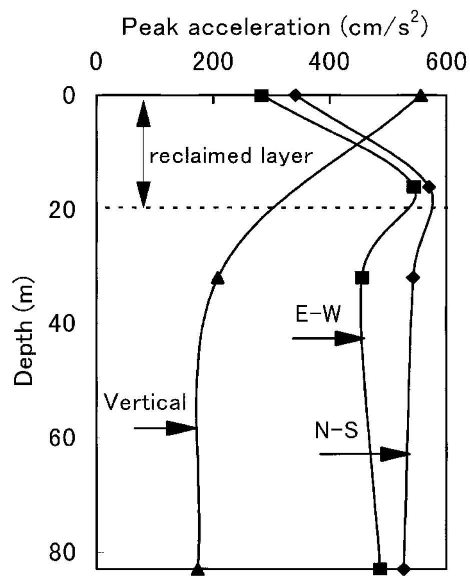

Figure 2. Distribution of peak accelerations in three components with depth.

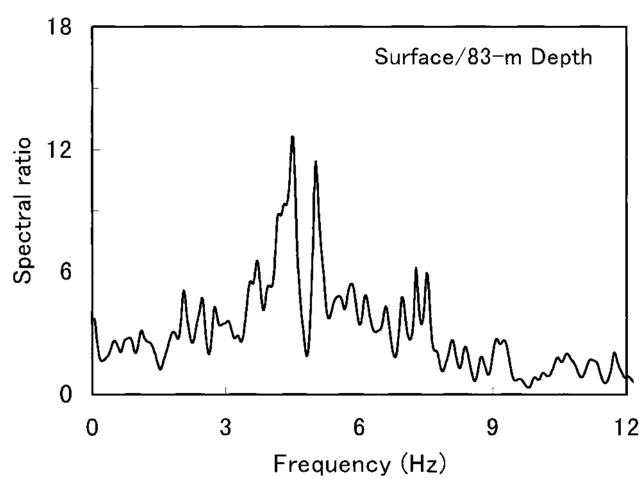

Figure 3. Spectral ratios of the vertical accelerations at the surface and 83-m depth.

the liquefied layers, which was manifested by a significant reduction of peak accelerations and an increase of effective periods of horizontal surface motions, as seen in Yang *et al.* (2000). For this reason, we consider that the large amplification of vertical motion observed at the array site may mainly involve *P* waves rather than long-period surface waves generated by diffraction effects, or *SV* waves if taking account of some possible *S*-*P* conversion. Furthermore, we consider that low velocity of *P* wave is associated with pore-water saturation of near-surface soils, because saturation strongly affects *P*-wave velocity but does not influence the propagation of S waves, as is demonstrated in this article.

The objective of this article is to present a possible mechanism to explain the aforementioned vertical amplification in detail, especially from the viewpoint of geotechnical engineering. To this end, first, we address the characteristics of *P*-wave velocity and Poisson's ratio in relation to pore-water saturation in surface soils, based on the concept of homogeneous pore fluid and Biot's theory of two-phase media (Biot, 1941, 1956). The analysis provides evidence that the near-surface soils at the array site were not completely water-saturated, which resulted in the low velocity of *P* waves. Then, we analyze a simple model to theoretically investigate the influence of soil saturation on the amplification of vertical motion. The problem considered involves an incompletely saturated soil layer subjected to vertical excitations at the bottom. Analytical solution for amplification factor is derived and numerical results are presented. Finally, we perform a simulation of the observed vertical motions at the array site, using a solid-fluid coupled finite element procedure. The results demonstrate the influence of saturation on the vertical amplification.

Site Characterization

The borehole array was installed in the northwest corner of Port Island, which is a reclaimed island on the southwest side of Kobe city. The site consists of reclaimed surface layers down to the depth of 19 m. The soil profile in the borehole is shown in Figure 4. The average *P*-wave velocity of the layer (from the surface to the depth of 12.6 m) is very low, around 590 m/sec. The groundwater level was at 2.4 m depth before the earthquake, and it dropped to the depth of 3.5 m after the earthquake (Shibata *et al.*, 1996). The low *P*-wave velocity is believed to be attributed to incomplete saturation of soils; that is, the soils are not completely saturated by water, there exist air inclusions in soils. Incomplete saturation is associated with the change of pore-fluid compressibility which has been found to significantly affect the *P*-wave velocity (Ishihara, 1967; Allen *et al.,* 1980; Kanema, 1997).

Because of groundwater, soils are often assumed to be a fully water-saturated porous two-phase material in geomechanics (e.g., Biot, 1941; Zienkiewicz *et al.*, 1980): the solid phase is soil skeleton and the fluid phase is pore-water filling the voids. In certain situations, however, near-surface soils may not be fully water-saturated, although the degree of saturation may be high. For example, incomplete saturation conditions can be caused by the change of season, fluctuating water tables, flooding, and recharge of groundwater. It would be of value to establish some relationships between *P*-wave velocity, Poisson's ratio, and the degree of saturation for shallow soils, which may help to evaluate *in situ* saturation of soils, as shown later.

P-Wave Velocity

Apparently, one key difference between fully water-saturated soils and incompletely saturated soils is pore fluid. For the latter, pore fluid is a mixture of water and air, while for the former, pore fluid is water only. The relative proportions of constituent volumes for incompletely saturated soils can be characterized by porosity n and the degree of saturation S_r as

$$n = \frac{V_v}{V_t} \qquad S_r = \frac{V_w}{V_v} \tag{1}$$

in which V_v, V_w are the volumes of pores and pore-water, respectively, and V_t is total volume. One typical case is when the degree of saturation is sufficiently high (e.g., higher than 90%) so that the air is embedded in pore-water in the form of bubbles. For this special case the concept of homogeneous pore fluid (Verruijt, 1969; Chang and Duncan, 1983) may be applied to the theory of two-phase media, and the bulk modulus of the homogeneous fluid K_f can be approximately expressed in terms of the degree of saturation as

$$K_f = \frac{1}{\dfrac{1}{K_w} + \dfrac{1 - S_r}{p_a}} \tag{2}$$

in which K_w is the bulk modulus of water and p_a is absolute fluid pressure. Figure 5 shows the variation of bulk modulus with air proportion $(1 - S_r)$. It is seen that even a very small amount of air in soil can drastically reduce the bulk modulus of fluid. For instance, at 100 kPa of absolute fluid pressure, the bulk modulus for $S_r = 99.97\%$ is less than one fifth of that for a fully saturated soil.

Introducing equation (2) into Biot's theory for wave propagation in porous media, the governing equations are given as

$$G\nabla^2\mathbf{u} + (\lambda + \alpha^2 M + G)\nabla e - \alpha M\nabla\zeta = \rho\ddot{\mathbf{u}} + \rho_f\ddot{\mathbf{w}} \tag{3}$$

$$\alpha M\nabla e - M\nabla\zeta = \rho_f\ddot{\mathbf{u}} + \frac{\rho_f}{n}\ddot{\mathbf{w}} + \frac{\eta}{k}\mathbf{w} \tag{4}$$

where $e = \mathrm{div}\mathbf{u}$ and $\zeta = -\mathrm{div}\mathbf{w}$, u and w are, respectively, the displacement vectors of solid skeleton and pore fluid with respect to solid phase; η is fluid viscosity; k is perme-

Depth	Soil Description	Accelerometer	P wave (m/sec)	S wave (m/sec)	Poisson's ratio
0.0 m – 2.0	Sandy gravel	0 m	260	170	0.127
2.0 – 5.0	Sandy gravel		330	170	0.319
5.0 – 12.6	Sandy gravel		780	210	0.461
12.6 – 19.0	Sand with gravel	16 m	1480	210	0.490
19.0 – 27.0	Alluvial clay		1180	180	0.488
27.0 – 33.0	Alluvial sand	32 m	1330	245	0.482
33.0 – 50.0	Sand with gravel		1530	305	0.479
50.0 – 61.0	Diluvial sand		1610	350	0.475
61.0 – 79.0	Diluvial clay		1610	303	0.482
79.0 – 83.0	sand with gravel	83 m	2000	320	0.487

Figure 4. Soil profile at the borehole site (not scaled).

ability (m^2); $\rho = (1 - n)\rho_s + n\rho_f$, ρ_s and ρ_f are mass densities of solid grains and pore fluid, respectively; λ and G are Lame constants of soil skeleton; α and M are parameters accounting for the compressibilities of grains and fluid. They can be given as

$$\alpha = 1 - \frac{K_b}{K_s} \quad M = \frac{K_s^2}{K_d - K_b}$$
$$K_d = K_s\left[1 + n\left(\frac{K_s}{K_f} - 1\right)\right] \tag{5}$$

in which K_s and K_b are bulk moduli of solid grains and skeleton, respectively; K_f is the bulk modulus of pore fluid, it is related to the bulk modulus of pore water, absolute fluid pressure and degree of saturation as described in equation (2).

Following similar procedures in Yang and Sato (1998a), equations (3) and (4) can be solved to yield two kinds of compressional waves traveling with different velocities (the fast and slow waves, respectively) and one shear wave. All the three types of waves are frequency-dependent and attenuated, and the influence of degree of saturation on each of them is different (Yang and Sato, 1998b). In low frequency range, to which the frequencies used in most field experiments such as crosshole method belong, only the fast compressional wave (referred to as P wave) and shear wave (S wave) exist, their velocities can be given as

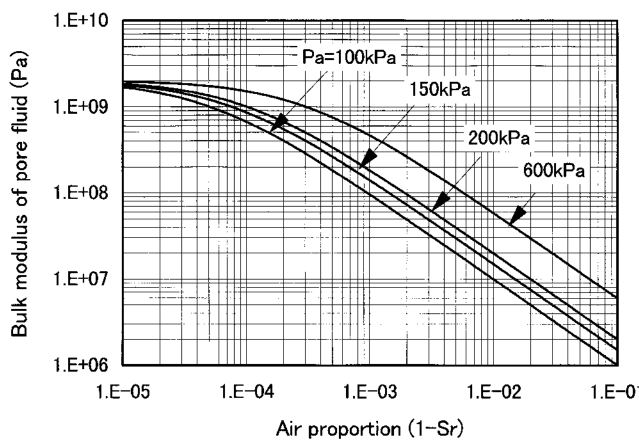

Figure 5. Influence of degree of saturation on the bulk modulus of pore fluid.

$$V_p = \sqrt{\frac{\lambda + 2G + \alpha^2 M}{\rho}} \qquad V_s = \sqrt{\frac{G}{\rho}} \tag{6}$$

Figure 6 shows the saturation effects on P-wave velocity for several types of soils in terms of stiffness. As expected, the *P*-wave velocity decreases substantially with even a slight decrease below full saturation. The velocity reaches maximum in the case of full saturation, about 1500 m/sec, while it drops to around 400 m/sec when the degree of saturation is 98%. For S waves, as indicated in equation (6), the influence of degree of saturation is negligible.

Poisson's Ratio

Poisson's ratio is one of important parameters to describe the elastic behavior of soils. Poisson's ratio for fully saturated soils is often assumed to be very close to 0.5 in geotechnical practice. However, due to the influence of degree of saturation on *P* waves, it is expected that Poisson's ratio may be affected by saturation as well. The evaluation of such influence is of interest because it would provide some additional information in identifying *in situ* saturation states, as shown later.

Obviously, with equation (6) Poisson's ratio can be determined from the ratio of *P*-wave velocity and *S*-wave velocity as

$$\nu = \frac{1}{2}\left(1 - \frac{G}{\lambda + \alpha^2 M + G}\right) \tag{7}$$

To evaluate the range of ν, introducing the Poisson's ratio for soil skeleton, which depends on the Lame constants of the skeleton as

$$\nu' = \frac{\lambda}{2(\lambda + G)} \tag{8}$$

Equation (7) may be given in an alternative form as

$$\nu = \frac{1}{2}\,\frac{\alpha^2 M/G + 2\nu'/(1 - 2\nu')}{\alpha^2 M/G + 1/(1 - 2\nu')}. \tag{9}$$

From this equation it can be readily shown that the range of ν is $\nu' \leqq \nu \leqq ½$. The upper limit may be reached for incompressible constituents ($\alpha = 1$, $1/M = 0$), and the lower bound is achieved when pore fluid is highly compressible ($K_f << G$).

By ignoring the compressibility of soil grains, which is a widely accepted assumption in soil mechanics, equation (9) can be reduced to the following form:

$$\nu = \frac{1}{2}\,\frac{K_f/nG + 2\nu'/(1 - 2\nu')}{K_f/nG + 1/(1 - 2\nu')}. \tag{10}$$

Further, for the case of complete saturation, equation (10) can be simplified by considering that for most soils the condition $\lambda + 2G << K_w/n$ is satisfied:

$$\nu \approx \frac{1}{2}\left(1 - \frac{nG}{K_w}\right). \tag{11}$$

Obviously, equation (11) is the Poisson's ratio for fully saturated soils usually used in geotechnical engineering as shown in Ishihara (1996).

Figure 7 shows the effects of degree of saturation on Poisson's ratio for several types of soils in terms of stiffness and absolute pore pressure, here ν' is taken to be 0.3, a typical value for most soils. Clearly, the influence of degree of saturation on Poisson's ratio is significant and that influence depends on soil stiffness and absolute pore pressure. In general, Poisson's ratio decreases with the increase of air proportion or the decrease of degree of saturation. The upper limit of Poisson's ratio is 0.5, which may be reached for fully saturated soft soils, while the lower bound is ν', which can be achieved in the relatively high air-saturation situation. Between the two limits, the variation of Poisson's ratio is little for soft soils, while the transition is large for soils with higher stiffness.

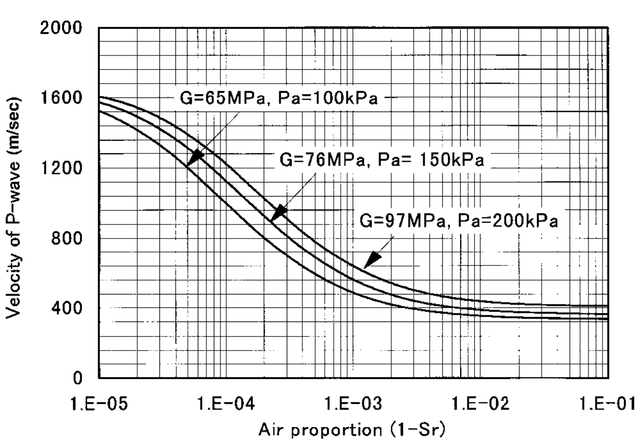

Figure 6. Effects of degree of saturation on *P*-wave velocity.

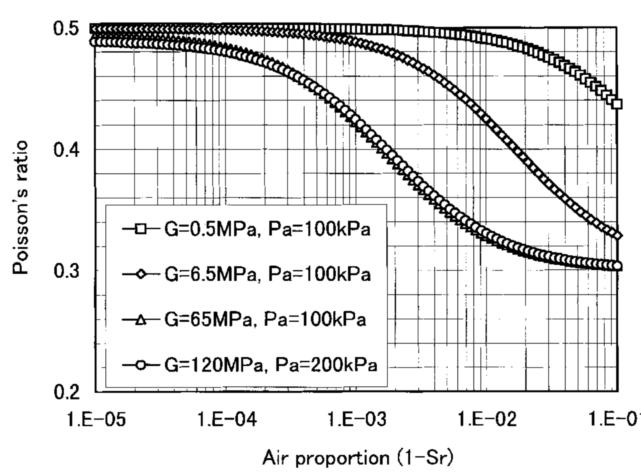

Figure 7. Effects of degree of saturation on Poisson's ratio.

Variations of *P*-Wave Velocity and Poisson's Ratio in Surface Soils

We have established some relationships among *P*-wave velocity, Poisson's ratio, and the degree of saturation of soils, and have demonstrated that both *P*-wave velocity and Poisson's ratio strongly depend on the degree of saturation. Based on these results, a schematic illustration of possible structures of *P*-wave velocity and Poisson's ratio in surface soil layers is given in Figure 8, by considering the variation of degree of saturation in vertical direction. With increasing depth, the saturation state of surface soils varies from low saturation to high saturation and finally to complete saturation at some depth. *P*-wave velocity dramatically increases from incomplete saturation to full saturation. As for Poisson's ratio, due to the increase of degree of saturation, it also increases with depth until the soils reach the state of full saturation, for which case the value of Poisson's ratio is close to 0.5; after that it tends to decrease with depth, because the stiffness of soils usually increases with depth gradually.

The discussion of the variations of *P*-wave velocity and Poisson's ratio in shallow soil layers has been supported by some field test data (Kitsunezaki, 1986; Kamei and Nakamura, 1992; Nigbor and Imai, 1994). Especially, the soil profile at the borehole array site, as shown in Figure 4, provides clear evidence. It is seen that *P*-wave velocity shows a great increase with depth, from 260 m/sec at the top to 2000 m/sec at the bottom. In particular, at the depth of 12.6 m there is a dramatic transition in *P*-wave velocity, from 780 m/sec to 1480 m/sec. The soil layers with low *P*-wave velocity below the water table to such depth are believed to be incompletely saturated. In addition, Poisson's ratio increases from 0.127 at the top to 0.490 at the depth of 12.6 m, below which it gradually decreases. This tendency is in good agreement with our theoretical prediction.

Theoretical Analysis of a Simple Model

So far we have discussed the characteristics of soil conditions in shallow layers and shown evidence of incomplete saturation in near-surface soils at the array site. To further investigate the effects of saturation on seismic vertical amplification, in this section we analyze an idealized problem based on Biot's theory of two-phase media. The simple model considered is shown in Figure 9. Vertical excitations, the time-dependent displacements, are applied at the bottom boundary of a soil layer. The surface of the layer is treated as pervious and stress-free, whereas the bottom of the layer is conventionally assumed to be impervious. The soils are assumed to be incompletely saturated with a small amount of air inclusions. For this one-dimensional problem, the governing equations (2) and (3) can be reduced to the following forms

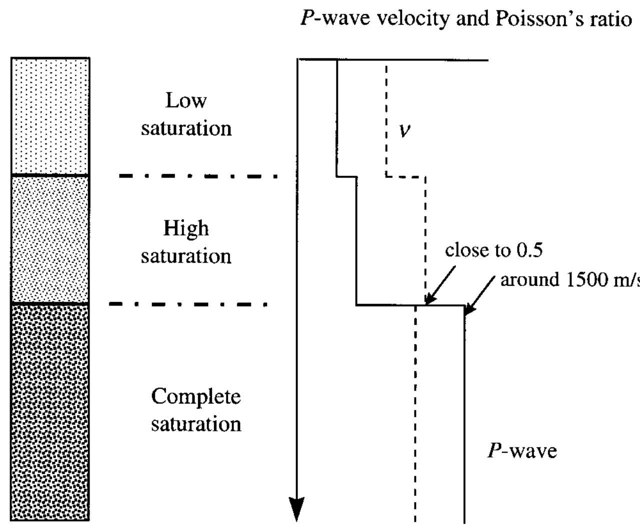

Figure 8. Variations of *P*-wave velocity, Poisson's ratio, and saturation in shallow layers.

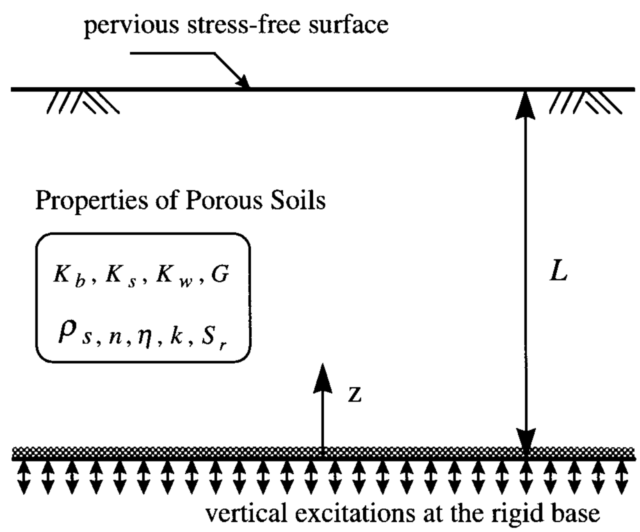

Figure 9. A soil layer subjected to vertical excitations at the bottom.

$$(\lambda + \alpha^2 M + 2G)\frac{\partial^2 u}{\partial z^2} + \alpha M \frac{\partial^2 w}{\partial z^2} = \rho \frac{\partial^2 u}{\partial t^2} + \rho_f \frac{\partial^2 w}{\partial t^2} \quad (12)$$

$$\alpha M \frac{\partial^2 u}{\partial z^2} + M \frac{\partial^2 w}{\partial z^2} = \rho_f \frac{\partial^2 u}{\partial t^2} + \frac{\rho_f}{n}\frac{\partial^2 w}{\partial t^2} + \frac{\eta}{k}\frac{\partial w}{\partial t} \quad (13)$$

The boundary conditions as stated above are given as

$$\text{At bottom, } z = 0: \quad u = U_0 e^{i\omega t},\ w = 0 \quad (14)$$

At surface, $z = L$:

$$p_f = 0, \sigma = 0 \tag{15}$$

where σ is total stress and p_f is pore fluid pressure. By enforcing the boundary conditions the solutions for displacements can be derived as (time factor $e^{i\omega t}$ is omitted)

$$u = \frac{U_0}{\delta_1 - \delta_2}\left(\delta_1 \frac{\cos[k_1(L - z)]}{\cos(k_1 L)} - \delta_2 \frac{\cos[k_2(L - z)]}{\cos(k_2 L)}\right) \tag{16}$$

$$w = \frac{U_0}{\delta_1 - \delta_2}\left(\frac{\cos[k_1(L - z)]}{\cos(k_1 L)} - \frac{\cos[k_2(L - z)]}{\cos(k_2 L)}\right) \tag{17}$$

where δ_1 and δ_2 are the roots of the following equation

$$A\delta^2 + B\delta + C = 0 \tag{18}$$

$$\begin{aligned} A &= \rho_f(\lambda + \alpha^2 M + 2G) - \rho\alpha M, \\ B &= (\lambda + \alpha^2 M + 2G)(\rho_f/n - i\eta/k\omega) - \rho M, \\ C &= \alpha M(\rho_f/n - i\eta/k\omega) - \rho_f M \end{aligned} \tag{19}$$

and k_1, k_2 are wave numbers for the two types of compressional waves, they are given by

$$k_1^2 = \frac{(K_{12}M_{21} - K_{22}M_{11} - iK_{12}\eta/k\omega)\omega^2}{K_{12}K_{21} - K_{11}K_{22}} \tag{20}$$

$$k_2^2 = \frac{(K_{11}M_{22} - K_{21}M_{12} - iK_{11}\eta/k\omega)\omega^2}{K_{11}K_{22} - K_{21}K_{12}} \tag{21}$$

in which K_{ij} and M_{ij} are the elements of the following matrices

$$[K] = \begin{bmatrix} (\lambda+\alpha^2 M+2G)\delta_1 + \alpha M & (\lambda+\alpha^2 M+2G)\delta_2 + \alpha M \\ \alpha M\delta_1 + M & \alpha M\delta_2 + M \end{bmatrix}$$

$$[M] = \begin{bmatrix} \rho\delta_1 + \rho_f & \rho\delta_2 + \rho_f \\ \rho_f\delta_1 + \rho_f/n & \rho_f\delta_2 + \rho_f/n \end{bmatrix}. \tag{22}$$

The details for the derivation of solutions can be found in Yang and Sato (1998c), in which the total stress and pore pressure are also given based on constitutive equations. The interest of this study is focused on motion amplification, which is readily defined here as the ratio of the solid displacement at any depth to the base displacement as

$$A_f = \frac{1}{\delta_1 - \delta_2}\left(\delta_1 \frac{\cos[k_1(L - z)]}{\cos(k_1 L)} - \delta_2 \frac{\cos[k_2(L - z)]}{\cos(k_2 L)}\right). \tag{23}$$

Figure 10 shows the variation of the amplitude of amplification factor at the surface with frequency. The soil properties, which are typical values of medium dense sands, are shown in Table 1. The thickness of the layer is assumed to be 15 m and the absolute fluid pressure p_a is assumed to be 150 kPa. Two cases of saturation, $S_r = 100\%$ and $S_r = 98\%$, are presented to show the effects of saturation. Even if the degree of saturation is only slight below full saturation, its impact on the amplification is significant. Both the amplitude and frequency content are strongly influenced by the degree of saturation. Compared with the case of full saturation, the amplification in the case of incomplete saturation is much greater in earthquake frequency range. In addition, it is noticed that the predominant frequency in the case of incomplete saturation is shifted toward the low frequency end; in other words, the predominant period is lengthened due to the partial saturation condition. This is reasonable since the air inclusion results in a dramatic decrease of *P*-wave velocity, as seen in Figure 6. In Figure 11 the distribution of amplification factors within the soil layer is shown for the two cases of saturation for the specific frequency of 5 Hz. Again, it is observed that the motion is amplified greatly when the soils are assumed as incompletely saturated, whereas in the case of full saturation, almost no am-

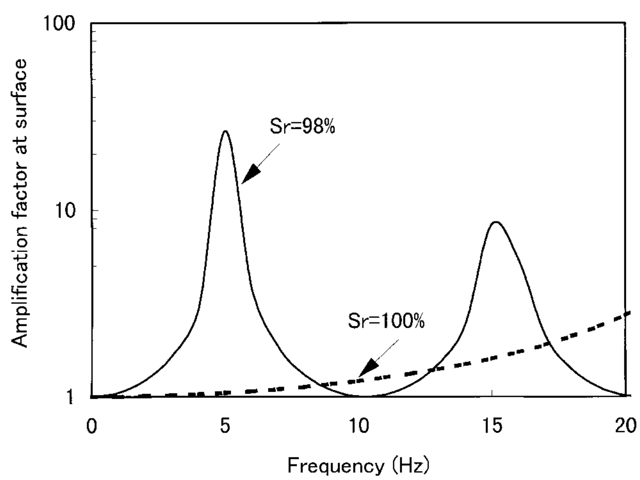

Figure 10. Effects of degree of saturation on amplification function.

Table 1
Soil Properties Used in Theoretical Analysis

Quantity	Value
Bulk modulus of solid skeleton	$K_b = 8.67 \times 10^7$ Pa
Bulk modulus of solid grains	$K_s = 3.6 \times 10^{10}$ Pa
Bulk modulus of water	$K_w = 2 \times 10^9$ Pa
Shear modulus of solid skeleton	$G = 6.5 \times 10^7$ Pa
Permeability	$k = 10^{-10}$ m^2
Viscosity	$\eta = 10^{-3}$ Pa s
Density of grains	$\rho_s = 2650$ kg/m^3
Porosity	$n = 0.37$

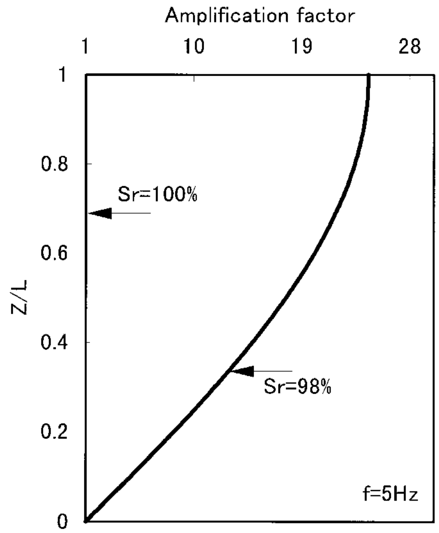

Figure 11. Distribution of amplification factor within the layer.

plification takes place (the amplification factor at the surface is around 1.05).

If we treat the amplification function for the case of incomplete saturation as the one which reflects the true condition of the site, while the incorrect amplification function is the one presumably obtained without considering such soil condition. These results suggest the need to carefully examine the condition of saturation in the study of vertical site amplification. Of course, the model considered here is simplified, in a real case the site is a multilayered system, more than one predominant frequencies may exist and the transfer function may also involve multiple vibration modes. However, the simple model does provide a direct picture of the effects of saturation on the vertical-motion amplification.

Numerical Simulation of Vertical Motions at the Array Site

In this section we extend the investigation from the simple model to the realistic site considered. We perform a simulation of the vertical motions at the borehole array site by including the effects of saturation. The numerical procedure used here is a solid-fluid coupled finite element procedure for response analysis of horizontally layered sites under multidirectional earthquake loading (Li *et al.*, 1998; Yang *et al.*, 2000). In this procedure, site response to horizontal and vertical base motions is assumed to be the consequence of the vertical propagation of shear waves and compression waves. The wave propagation and transient pore-fluid movement in soil system are coupled through the generalized Biot's formulation (e.g., Zienkiewicz and Shiomi, 1984; Prevost, 1986) and advanced soil models (e.g., Wang *et al.*, 1990; Herrmann *et al.*, 1983). The predictive capability of the procedure has been verified to some extent using laboratory centrifuge tests (Sivathasan *et al.*, 1998) and field observations from the 1986 Lotung earthquake (Li *et al.*, 1998). Using this procedure, we investigated the liquefaction-induced nonlinear effects on horizontal motions at the site considered in this article (Yang *et al.*, 2000). The computed results showed reasonable agreements with the field records. Details of the procedure, soil models integrated, and numerical implementation are given in the corresponding references noted earlier. Our intention here is to simulate the vertical motions at the array site by incorporating the effects of saturation into this procedure.

In conventional coupled site response analyses, soils below the water table are often assumed to be completely saturated. It is recognized that the influence of saturation on vertical site amplification has not yet drawn much attention, and it remains difficult to incorporate the effects of partial saturation. Based on our previous discussions, we make an attempt to investigate such effects on vertical amplification. One key issue is to determine the degree of saturation (or the compressibility of pore fluid) of near-surface soils. For the array site considered, as indicated earlier, it is reasonable to assume that soils below the water table (the depth of 2.4 m) are incompletely saturated to the depth of 12.6 m. Within this unsaturated range, soils are composed of two layers which have the average *P*-wave velocities of 330 m/sec and 780 m/sec, and Poisson's ratios of 0.319 and 0.461, respectively. Using the relationships established among the degree of saturation, *P*-wave velocity and Poisson's ratio, we may estimate that the average values of degree of saturation for the two layers are around 98% and 99.96%. Then, the bulk modulus of pore fluid can be modified according to equation (2) and be incorporated into the numerical procedure. As for the soils above the water table, conventionally, they are approximately assumed as one-phase media (namely, dry state), whereas the soils below the depth of 12.6 m can be treated as fully water saturated.

The simulation is limited to the top 83 m of the deposit in which the soils were characterized in detail and the accelerometers were also embedded (see Figure 4). The soil model and model parameters selected for the deposit were described in Yang *et al.* (2000). The early parts (from 0 to 10 sec) in the acceleration records at the depth of 83 m serve as the input motions. These parts in vertical component, as seen in Figure 1, are considered to contain most high-frequency *P* waves (probably including some *P* waves converted from *S* waves at the layer boundaries below 83 m). The method suggested by Tsai (1969) for treatment of boundary conditions between the soil deposit and underlying rock base has been employed in the formulation. That method allows both equilibrium and continuity conditions at the boundary to be satisfied not only when the input motions are specified at outcropping rock but also when the motions are directly taken from borehole records. To compare with the incomplete saturation case, we also conduct a conventional analysis, which assumes that the soils immediately below the water table are fully saturated (S_r = 100%). All input parameters in both analyses are identical except the degrees of saturation in the near-surface layers as indicated earlier.

Figure 12 shows the computed vertical acceleration-time histories at the ground surface for the two cases of saturation (denoted as incomplete and complete saturation, respectively). The acceleration response spectra with a damping factor of 5% is shown in Figure 13 for these two cases. Figure 14 shows the computed distributions of peak accelerations with depth for the two cases, together with the recorded peak values. While both simulated surface motions are in general very similar to the field records, all the results clearly indicate that the incomplete saturation of near-surface soils, as expected, can cause a larger vertical site amplification. The surface peak acceleration is 430 cm/sec^2 in the case of complete saturation, whereas it increases to 531 cm/sec^2 even if very slight incomplete saturation exists in near-surface layers. Similarly, the difference in peak acceleration response is as large as 250 cm/sec^2, which takes place at the period around of 0.15 sec. Figure 15 shows the spectral ratios of vertical motions at the surface and 83-m depth in the case of incomplete saturation, along with the ratios for recorded motions. Although there are some discrepancies between the simulation and observation, probably due to the uncertainties involved in the analysis and the limitations of the procedure, the calculated ratios match the overall trend of the observed ones very well, and the simulation is in reasonable agreement with the observation. Both calculated and

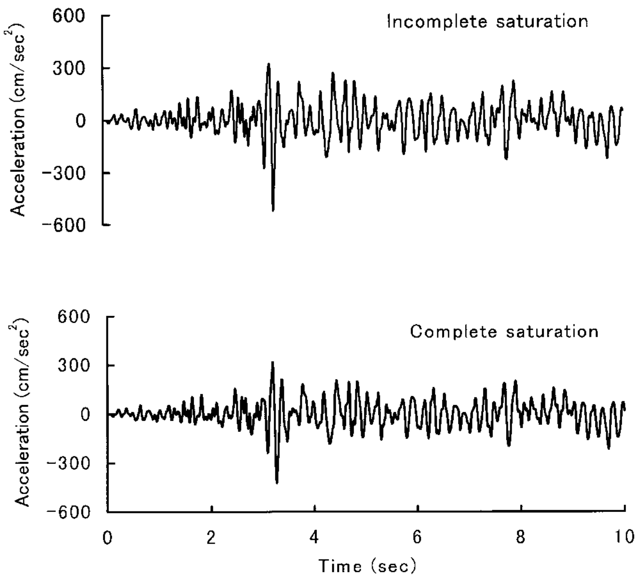

Figure 12. Simulated acceleration-time histories at the surface for two cases of saturation.

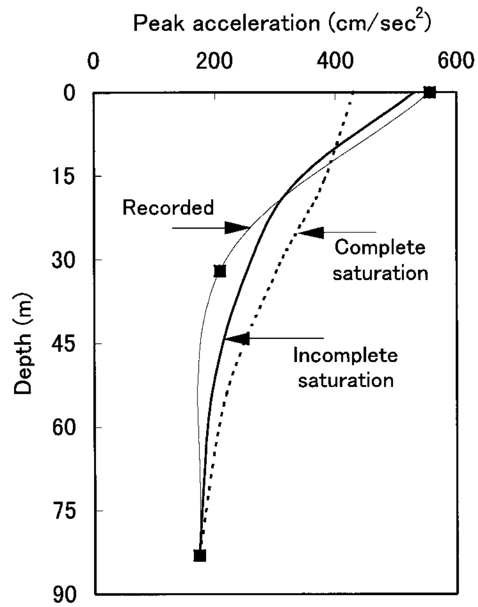

Figure 14. Distribution of peak accelerations with depth for two cases of saturation.

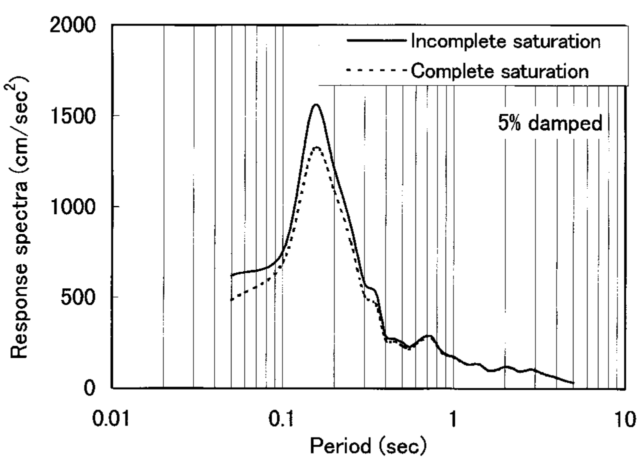

Figure 13. Ground surface response spectra for two cases of saturation.

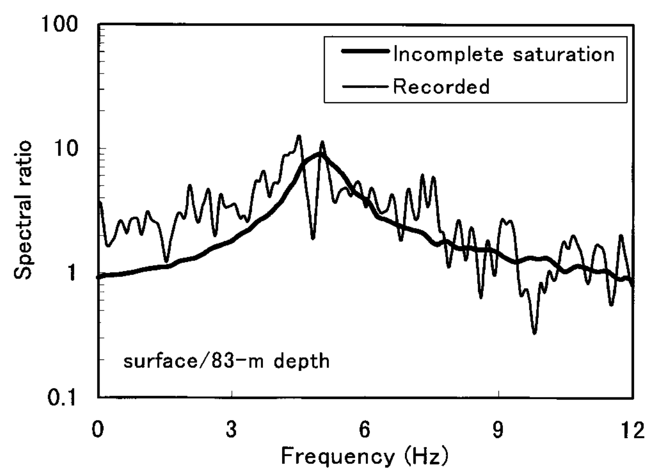

Figure 15. Simulated and recorded spectral ratios of vertical motions at the surface and 83-m depth.

observed large amplification took place at frequencies around of 4.5 to 5.5 Hz.

Conclusions

In this article, we present a possible mechanism to explain the large amplification of vertical motion observed at Port Island, Kobe, during the 1995 Hyogo-ken Nanbu (Kobe) earthquake. The mechanism, amplification of *P* waves caused by incomplete saturation of near-surface soils, is explained using the concept of homogeneous pore fluid and Biot's theory of two-phase media.

We discussed the characteristics of *P*-wave velocity, Poisson's ratio, and the degree of saturation in near-surface soil layers. It is shown that a small change in the degree of saturation can cause dramatically change in *P*-wave velocity and Poisson's ratio, whereas the influence of degree of saturation on *S* waves is negligible. The established relationships among these properties would be useful in estimating *in situ* pore-water saturation of soils, as demonstrated for the array site considered.

The analytical study for the simple model clearly indicates that the degree of saturation may produce substantial influence on vertical-motion amplification, both amplitude and frequency content. The simulation for the array site, through a solid-fluid coupled numerical procedure and by including the effects of saturation, demonstrates the mechanism of large vertical amplification caused by incomplete saturation of near-surface soils.

Vertical-component motions may be significantly affected by pore-water saturation of shallow soil layers, suggesting that we may need to carefully examine the condition of saturation in the study of vertical site amplification.

Acknowledgments

The authors thank Art McGarr, Hsi-Ping Liu, and an anonymous reviewer for valuable comments and suggestions which helped to improve the manuscript. Thanks also go to X. S. Li for useful discussions on the numerical procedure for site-response analysis. We acknowledge the financial support provided by the Ministry of Education and Science, Japan, via the program of Center of Excellence (to J. Yang).

References

Allen, F. A., F. E. Richart Jr, and R. D. Woods (1980). Fluid wave propagation in saturated and nearly saturated sands, *J. Geotech. Eng. ASCE* **106,** 235–254.

Aguirre, J., and K. Irikura (1997). Nonlinearity, liquefaction, and velocity variation of soft soil layers in Port Island, Kobe, during the Hyogo-ken Nanbu earthquake, *Bull. Seism. Soc. Am.* **87,** 1244–1258.

Biot, M. A. (1941). General theory of three-dimensional consolidation, *J. Appl. Mech.* **15,** 155–164.

Biot, M. A. (1956). Theory of propagation of elastic waves in a fluid saturated porous solid, *J. Acoust. Soc. Am.* **28,** 168–191.

Boore, D. M., and C. E. Smith (1999). Analysis of earthquake recordings obtained from the seafloor earthquake measurement system (SEMS) instruments deployed off the coast of southern California, *Bull. Seism. Soc. Am.* **89,** 260–274.

Chang, C. S., and J. M. Duncan (1983). Consolidation analysis for partly saturated clay by using an elastic-plastic effective stress-strain model, *Int. J. Numer. Anal. Methods Geomech.* **7,** 39–56.

Herrmann, L. R., J. S. DeNatale, and Y. F. Dafalias (1983). Numerical implementation of cohesive soil bounding surface plasticity model, *Civil Eng. Lab. Rept. CR 83.010,* Naval Construction Battalion Center.

Ishihara, K. (1967). Propagation of compressional waves in a saturated soil, in *Proceedings of the International Symposium on Wave Propagation and Dynamic Properties of Earth Materials,* 451–467.

Ishihara, K. (1996). *Soil Behavior in Earthquake Geotechnics,* Oxford University Press, New York.

Kamei, K., and Y. Nakamura (1992). Estimation of velocity of elastic waves based on SPT, *Soils and Foundations* (Japanese version) **40,** 41–46.

Kanema, T. (1997). Effect of air saturation on velocity and attenuation of elastic waves in water-filled sands with partial air saturation, *Geophysical Exploration* **50,** 229–245 (in Japanese).

Kawase, H. (1996). On the strong ground motion during the Hyogo-ken Nanbu earthquake of 1995, in *Proceedings of the Annual Conference of Architectural Institute of Japan,* 7–8 (in Japanese).

Kawase, H., and Y. Hayashi (1996). Strong motion simulation in Chuo Ward, Kobe, during the Hyogo-ken Nanbu earthquake of 1995 based on the inverted bedrock motion, *J. Struc. Constr. Eng. AIJ,* **480,** 67–76 (in Japanese).

Kitsunezaki, C. (1986). Velocity and attenuation of elastic waves in water-filled sand layers with partial gas saturation and their practical significance, *Geophysical Exploration* **39,** 42–59 (in Japanese).

Kokusho, T., and M. Matsumoto (1999). Nonlinear site amplification in vertical array records during Hyogo-ken Nanbu earthquake, *Soil and Foundations,* (Special Issue No. 2), 1–9.

Lermo, J., and J. Chavez-Garcia (1993). Site effect evaluation using spectral ratios with only one station, *Bull. Seism. Soc. Am.* **83,** 1574–1594.

Li, X. S., C. K. Shen, and Z. L. Wang (1998). Fully coupled inelastic site response analysis for 1986 Lotung earthquake, *J. Geotech. Geoenviron. Eng. ASCE***124,** 560–573.

Nakamura, Y. (1989). A method for dynamic characteristics estimation of subsurface using microtremor on the ground surface, *QR Railway Tech. Res. Inst.* **30,** 25–33.

Nigbor, R. L., and Y. Imai (1994). The suspension P-S velocity logging method, in *Geophysical Characterization of Sites,* Special Volume by Technical Committee 10 for XIII International Conference on Soil Mechanics and Foundation Engineering, 57–61.

Pitarka, A., K. Irikura, T. Iwata, and H. Sekiguchi (1998). Three-dimensional simulation of the near-fault ground motion for the 1995 Hyogo-ken Nanbu (Kobe), Japan, earthquake, *Bull. Seism. Soc. Am.* **88,** 428–440.

Prevost, J. H. (1986). Effective stress analysis of seismic site response, *Int. J. Numer. Anal. Methods Geomech.* **10,** 653–665.

Sato, K., T. Kokusho, M. Matsumoto, and E. Yamada (1996). Nonlinear seismic response and soil property during strong motion, *Soils and Foundations* (Special Issue), 41–52.

Shibata, T., F. Oka, and Y. Ozawa (1996). Characteristics of ground deformation due to liquefaction, *Soils and Foundations* (Special Issue), 65–80.

Sivathasan, K., G. H. Paulino, X. S. Li, and K. Arulanandan (1998). Validation of site characterization method for the study of dynamic pore pressure response, *Geotechnical Special Pub. 75,* 469–481.

Theodulidis, N. P., and P. Y. Bard (1995). Horizontal to vertical spectral ratio and geological conditions: an analysis of strong motion data from Greece and Taiwan (SMART-1), *Soil Dyn. Earthquake Eng.* **14,** 177–197.

Trifunac, M. D., and M. I. Todorovska (1996). Nonlinear soil response—1994 Northridge, California, Earthquake, *J. Geotech. Eng. ASCE* **122,** 725–735.

Tsai, N. C. (1969). Influence of local geology on earthquake ground motion, *Ph.D. Thesis,* California Institute of Technology, Pasadena, California.

Verruijt, A. (1969). Elastic storage of aquifers, in *Flow Through Porous Media,* R. J. M. de Weist (Editor), Academic Press, London.

Wang, Z. L., Y. F. Dafalias, and C. K. Shen (1990). Bounding surface hypoplasticity model for sand, *J. Eng. Mech. ASCE* **116,** 983–1001.

Yang, J., and T. Sato (1998a). Influence of viscous coupling on seismic reflection and transmission in saturated porous media, *Bull. Seism. Soc. Am.* **88,** 1289–1299.

Yang, J., and T. Sato (1998b). On the velocity and damping of elastic waves in nearly saturated soils, in *Proceedings of the 33rd Japan National Conference on Geotechnical Engineering,* Paper No. 576.

Yang, J., and T. Sato (1998c). Seismic response of a partially saturated sand layer, in *Proceedings of the 10th Japan Earthquake Engineering Symposium,* 799–804.

Yang, J., T. Sato, and X. S. Li (2000). Nonlinear site effects on strong ground motion at a reclaimed island, *Can. Geotech. J.* **37(1),** in press.

Zienkiewicz, O. C., C. T. Chang, and P. Bettes (1980). Drained, undrained, consolidating and dynamic behavior assumptions in soils, *Geotechnique* **30,** 385–395.

Zienkiewicz, O. C., and T. Shiomi (1984). Dynamic behaviour of saturated porous media: the generalized Biot formulation and its numerical solution, *Int. J. Numer. Anal. Methods Geomech.* **8,** 71–96.

Disaster Prevention Research Institute
Kyoto University
Gokasho, Uji, Kyoto 611-0011
Japan
yang@catfish.dpri.kyoto-u.ac.jp
(J. Y.)

Manuscript received 24 May 1999.